JOURNAL OF GEOPHYSICAL RESEARCH, VOL. 111, B08409, doi:10.1029/2005JB003963, 2006

Microblock rotations and fault coupling in SE Asia triple junction (Sulawesi, Indonesia) from GPS and earthquake slip vector data

Anne Socquet,[1,2] Wim Simons,[1] Christophe Vigny,[3] Robert McCaffrey,[4] Cecep Subarya,[5] Dina Sarsito,[6] Boudewijn Ambrosius,[1] and Wim Spakman[7]

Received 19 July 2005; revised 31 March 2006; accepted 23 May 2006; published 31 August 2006.

[1] The island of Sulawesi, eastern Indonesia, is located within the triple junction of the Australian, Philippine, and Sunda plates and accommodates the convergence of continental fragments with the Sunda margin. We quantify the kinematics of Sulawesi by modeling GPS velocities and earthquake slip vectors as a combination of rigid block rotations and elastic deformation around faults. We find that the deformation can be reasonably described by a small number of rapidly rotating crustal blocks. Relative to the Sunda Plate, the southwestern part of Sulawesi (Makassar Block) rotates anticlockwise at ~1.4°/Myr. The northeastern part of Sulawesi, the Bangai-Sula domain, comprises three blocks: the central North Sula Block moves toward the NNW and rotates clockwise at ~2.5°/Myr, the northeastern Manado Block rotates clockwise at ~3°/Myr about a nearby axis, and East Sulawesi is pinched between the North Sula and Makassar blocks. Along the boundary between the Makassar Block and the Sunda Plate, GPS measurements suggest that the trench accommodates ~15 mm/yr of slip within the Makassar Strait with current elastic strain accumulation. The tectonic boundary between North Sula and Manado blocks is the Gorontalo Fault, moving right laterally at about 11 mm/yr and accumulating elastic strain. The 42 mm/yr relative motion between North Sula and Makassar blocks is accommodated on the Palu-Koro left-lateral strike-slip fault zone. The data also indicate a pull-apart structure in Palu area, where the fault shows a transtensive motion and may have a complex geometry involving several active strands. Sulawesi provides a primary example of how collision can be accommodated by crustal block rotation instead of mountain building.

Citation: Socquet, A., W. Simons, C. Vigny, R. McCaffrey, C. Subarya, D. Sarsito, B. Ambrosius, and W. Spakman (2006), Microblock rotations and fault coupling in SE Asia triple junction (Sulawesi, Indonesia) from GPS and earthquake slip vector data, *J. Geophys. Res.*, *111*, B08409, doi:10.1029/2005JB003963.

1. Introduction

[2] Relative motions between major, fast moving plates can sometimes be accommodated within a complex deforming zone that involves microblocks rotating rapidly about nearby poles (e.g., Cascadia, Marianas, Vanuatu, Papua New Guinea, New Zealand, Tonga) [*McCaffrey et al.*, 2000; *Kato et al.*, 2003; *Calmant et al.*, 2003; *Wallace et al.*, 2004, 2005], resulting in complex plate interactions. The boundaries between these rotating microplates are often the sites of major collisional orogenies, subduction zones, rift systems, and rapidly slipping transform faults. Accurate assessment of the kinematics of these convergent plate boundary microblocks, by using Global Positioning System (GPS) techniques for example, may help us help us resolve long-standing questions about the forces driving microplate rotation.

[3] Because the triple junction between the Philippine Sea, Australian, and Sunda plates in Southeast Asia is highly seismically active and is characterized by rapid rotations of small blocks revealed by both geological and kinematic studies [*Fitch and Hamilton*, 1974; *Hamilton*, 1972; *Kreemer et al.*, 2000; *Silver et al.*, 1983a; *Silver and Moore*, 1978; *Simons et al.*, 2000; *Stevens et al.*, 1999; *Vigny et al.*, 2002; *Walpersdorf et al.*, 1998a, 1998b] (Figure 1), it constitutes a type example of how a collision can be accommodated by block rotation instead of mountain building. However, to more fully understand this process, a more precise description of these microblock's motions and a better understanding of the main active structures of the

[1]Department of Earth Observation and Space Systems, Delft University of Technology, Delft, Netherlands.
[2]Department of Earth and Space Sciences, University of California, Los Angeles, California, USA.
[3]Laboratoire de Géologie de l'Ecole Normale Supérieure, UMR CNRS 8538, Paris, France.
[4]Department of Earth and Environmental Sciences, Rensselaer Polytechnic Institute, Troy, New York, USA.
[5]National Coordination Agency for Surveys and Mapping, Cibinong, Indonesia.
[6]Geodesy Research Group, Faculty of Civil and Environmental Engineering, Institute of Technology Bandung, Bandung, Indonesia.
[7]Faculty of Earth Sciences, Utrecht University, Utrecht, Netherlands.

0148-0227/06/2005JB003963$09.00

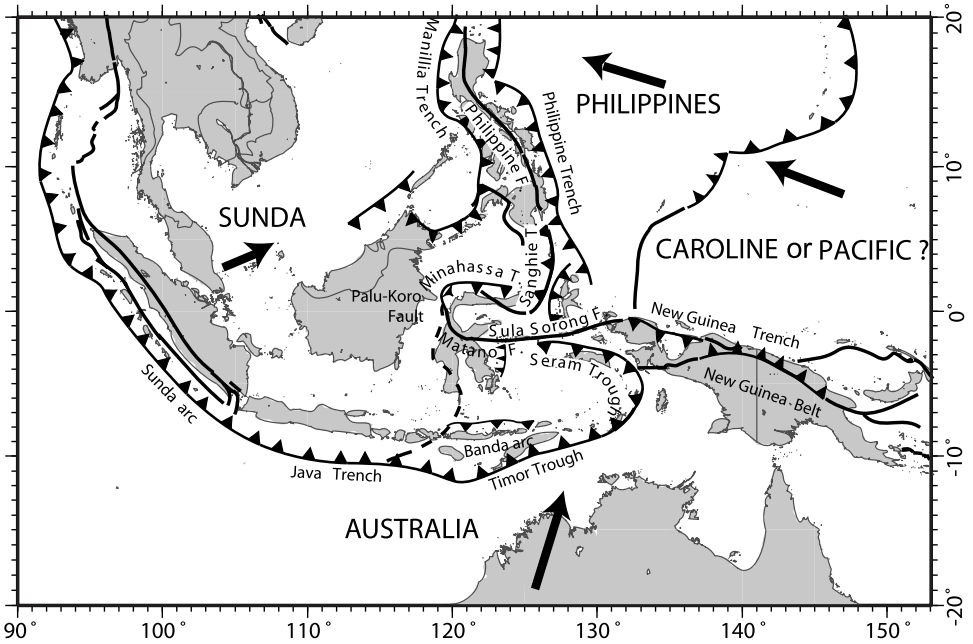

Figure 1. Structural map of the Sunda–Australia–Philippine–Pacific plates junction area. Arrows depict the far-field velocities of the plates with respect to Eurasia. Fault traces are adapted from *Hamilton* [1979].

area are necessary. The purpose of this paper study is to define the deformation of the Sulawesi area utilizing geodetic and seismological data. Using a decade of GPS measurements, we estimate the kinematics and likely boundaries of the micro blocks. We also examine the active faults of Sulawesi (e.g., Palu-Koro and Gorontalo strike-slip faults) in detail to quantify their interseismic behavior and assess their contributions to seismic hazards. Toward these ends, we model our GPS velocities and earthquake slip vector azimuths with a combination of rigid block rotations [*Morgan*, 1968; *Peltzer and Saucier*, 1996] and elastic deformation due to locking on the faults separating the blocks [*Okada*, 1985, 1992; *Savage*, 1983; *Savage and Burford*, 1973]. This simultaneous inversion results in Euler vectors describing rigid block rotation in addition to degree of coupling on the faults.

2. Geodynamic Setting

2.1. Present-Day Kinematics

[4] According to the NUVEL-1A plate motion model, the triple junction of Southeast Asia is a trench-trench-fault (T-T-F) type between the Eurasian (or Sunda), Australian, and Philippine plates [*DeMets et al.*, 1990, 1994] (Figure 1). The Australian and Philippine plates subduct beneath the Eurasia (or Sunda) Plate at rates of 75 and 90 mm/yr, respectively. The E-W trending Australia–Philippine Sea/Pacific boundary zone that extends from eastern Indonesia through New Guinea accommodates the relative plate motion by transpressive faulting and tectonic block rotation [*Tregoning et al.*, 1998, 1999, 2000; *Stevens et al.*, 2002; *Wallace et al.*, 2004]. GPS measurement in Indonesia have helped considerably to refine the plate kinematics of Southeast Asia [*Puntodewo et al.*, 1994; *Tregoning et al.*, 1994; *Genrich et al.*, 1996, 2000; *Prawirodirdjo et al.*, 1997, 2000; *Michel et al.*, 2001; *Bock et al.*, 2003]. In particular, GPS velocities revealed that the Eurasian Plate does not include Southeast Asia, but instead the separate Sunda Plate moves at about 10 mm/yr eastward relative to Eurasia [*Chamot-Rooke and Le Pichon*, 1999; *Michel et al.*, 2001; *Simons et al.*, 1999]. Studies based on denser GPS arrays in Sulawesi reveal even finer detail on block-like motions, for example, rapid clockwise rotation of the northern part of the Sulawesi Island, named the Sula Block, with respect to the Sunda Block [*Walpersdorf et al.*, 1998a, 1998b; *Stevens et al.*, 1999]. The latest study, based on 100+ sites in SE Asia, shows that deformation affects both the East Borneo and Sulawesi areas, while southern Sulawesi in particular, also moves independently of the Sunda Plate (W. J. F. Simons et al., A decade of GPS measurements in SE Asia: (Re)defining Sundaland and its boundaries, unpublished manuscript, 2005, hereinafter referred to as Simons et al., unpublished manuscript, 2005). These studies show that Sulawesi is clearly not a part of the Sunda Plate, but instead is itself broken into multiple microblocks accommodating complex deformation.

2.2. Regional Active Structures

[5] The active structures of the Sulawesi area show complex patterns of faulting [*Hall*, 2002; *Hall and Wilson*, 2000] (Figure 1). The Sunda Plate is bounded to the south by the Sunda-Banda arc which is associated with the northward subduction of the Australian Plate. Subduction of the Australian Plate at the Java Trench evolves into collision with Australia along the Timor Trough south of Sulawesi [*McCaffrey and Abers*, 1991]. Highly oblique convergence (~110 mm/yr) between the Pacific (or Caroline after [*Weissel and Anderson*, 1978]) and the Australian plates is accommodated in western New Guinea where shortening and left-lateral shear are distributed among

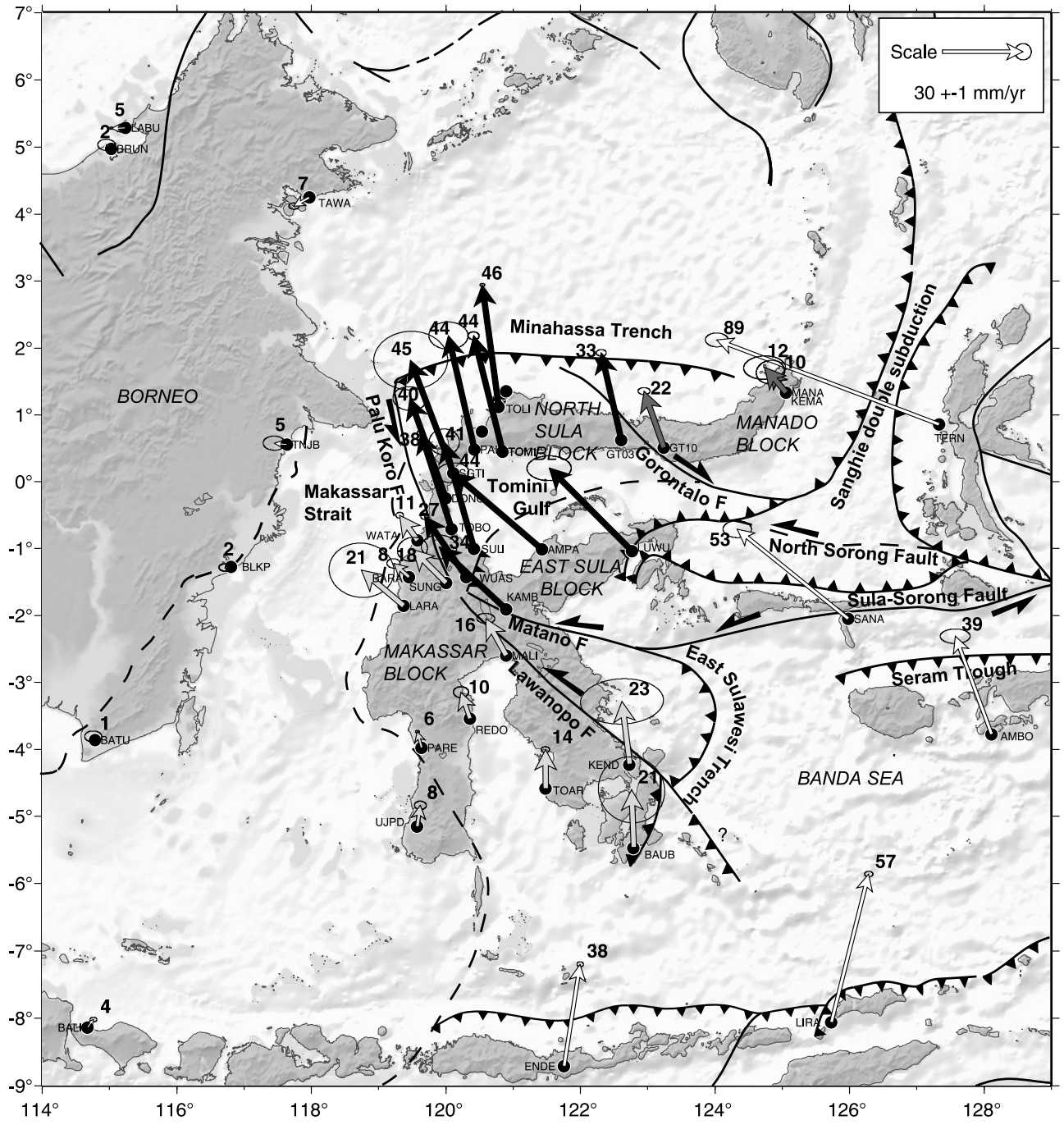

Figure 2. GPS velocities of Sulawesi and surrounding sites with respect to the Sunda Plate. Grey arrows belong to the Makassar Block, black arrows belong to the northern half of Sulawesi, and white arrows belong to non-Sulawesi sites (99% confidence ellipses). Numbers near the tips of the vectors give the rates in mm/yr. The main tectonic structures of the area are shown as well.

several tectonic boundaries [*McCaffrey and Abers*, 1991; *Puntodewo et al.*, 1994; *Stevens et al.*, 2002]. Faults in New Guinea continue to the west to the Seram Trough and to the Sula-Sorong Fault that continues into Sulawesi. In the Philippines, the oblique convergence between the Sunda and Philippine plates is accommodated by partitioning of the slip between the Philippine Trench and the Philippine Fault [*Aurelio*, 2000; *Fitch*, 1972]. The Manila-Philippine trench system (Figure 1) undergoes trench-normal convergence [*Rangin et al.*, 1999] while left-lateral strike slip is taken up on the Philippine Fault [*Barrier et al.*, 1991].

[6] The central part of the Southeast Asia triple junction coincides with Sulawesi (Figure 2). The northern part of the island, is colliding with the Sunda Plate [*Rangin*, 1989; *Silver et al.*, 1983a, 1983b]. This relative motion is accommodated by left-lateral strike-slip motion along the Matano/

Lawanopo Fault (the western continuation of the Sula-Sorong Fault [*Hinschberger et al.*, 2000]) which continues to the Palu–Koro Fault in the north, which then connects to the Minahassa Trench where subduction occurs (Figure 2). The Gorontalo strike-slip fault cuts the northern arm of Sulawesi and may connect to the Minahassa Trench. At the eastern termination of the Minahassa Trench, the Sangihe double subduction zone accommodates convergence between the Philippine Plate and Sulawesi across the Molucca Sea (Figure 2).

[7] The main active structure in Sulawesi is the Palu-Koro Fault and its southeast continuation to the Matano Fault and/or Lawanopo Fault. The Palu-Koro Fault bisects the island: the Makassar Block on the southwest and the North Sula Block on the northeast. GPS shows that the total motion across the fault is around 4 cm/yr. If this slip occurs on one single fault locked at depth [*Stevens et al.*, 1999; *Walpersdorf et al.*, 1998c], then it should produce at least one magnitude 7 earthquake every 100 years [*Wells and Coppersmith*, 1994]. This history of earthquakes is not seen in trenching in the Palu area [*Bellier et al.*, 2001], which poses a problem for reconciling neotectonics with the present-day geodetic rates.

3. GPS Velocity Field of the Triple Junction Area

3.1. GPS Measurements

[8] The first GPS measurements in Sulawesi took place in 1992 [*Bock et al.*, 2003] at which time detailed transects were also established across the Palu-Koro and Gorontalo faults [*Stevens et al.*, 1999]. Concurrently, in the GEODYSSEA project, a network of about 40 geodetic points covering an area of 4000 by 4000 km in Southeast Asia was installed and measured between 1994 and 1998 [*Michel et al.*, 2001]. In Sulawesi, the GPS network has been increased from the original eight GEODYSSEA sites in 1994 to more than 30 by 2003, plus 25 additional transect points across the Palu-Koro and Gorontalo faults. This network has been remeasured yearly since 1996. Since 1999, six continuous GPS stations have been installed mainly to study the transient behavior of the Palu-Koro Fault.

3.2. GPS Processing

3.2.1. Regional Processing

[9] The Sulawesi GPS data (campaign and continuous measurements) have been included in regional processing covering the entire Southeast Asia (Simons et al., unpublished manuscript, 2005). The station daily positions were computed with GIPSY software [*Blewitt et al.*, 1988], applying the PPP strategy to the ionosphere-free combination of the zero-differenced GPS dual-frequency observables at 5 min intervals, with a cutoff angle of 15°. Tropospheric delays and gradients were estimated at each interval. The processing included ocean loading parameters [*Scherneck*, 1991], variations of the antennae phase centers (National Geodetic Survey (NGS) [*Mader*, 1998]), precise satellite orbits and clocks, as well as Earth orientation parameters distributed by the Jet Propulsion Laboratory (JPL). Finally, the individual PPP solutions were merged into a daily network solution after which the ambiguities were fixed to integer values. These daily network solutions were combined into weekly or campaign-averaged solutions. The daily coordinate repeatabilities for the Sulawesi network have an internal accuracy of about 2 and 5 mm for the east and north positions and 9 mm for the height. These errors are slightly higher than those of the included IGS network, and can be explained by the less ideal site conditions (sky visibility and multipath issues) in Sulawesi. The 23 IGS stations included in the data set allowed us to project each multiday averaged solution onto the ITRF-2000 reference frame [*Altamimi et al.*, 2002], by applying seven-parameter Helmert transformations to their positions. The coordinate residuals between the projected and the predicted ITRF-2000 positions at each analyzed epoch exhibit stable RMS values of about 2 to 3 mm for the east and north, and 8 mm for the vertical position. The sites velocities were estimated by computing a linear fit through all the ITRF-2000 mapped coordinate time series, while excluding any epochs that were clearly disturbed by seismic events. The coordinate residuals with respect to the linear trend at each analyzed epoch have 3-D RMS values of 2, 3 and 8 mm for east, north, and up. The differences between the estimated and the ITRF-2000 velocities for the IGS stations used for the mapping have RMS values of 0.6, 0.7 and 2.5 mm/yr, respectively, indicating that the local velocity estimates are consistently computed in a stable reference frame. The uncertainties of the horizontal velocity vectors in Sulawesi range from 0.5 to 3.0 mm/yr, depending on the number of sessions or campaigns and on the total time span between first and last occupation at each site.

3.2.2. Palu Transect Relative Processing

[10] The main objective of the Palu transect study is to estimate the velocity variations across the Palu-Koro Fault with high relative accuracy. Therefore we follow a different observation and processing strategy: each year the WATA station was taken as a continuously recording reference and the other transect sites were each occupied for 24 hours or more. The positions of all the network sites were computed simultaneously with respect to WATA, following a fiducial network strategy which provides two important advantages. First, since the network is small (diameter of 60 km, no IGS sites included), almost all the ambiguities can be fixed. Second, there is no need to map the network into a global reference frame. The small network aperture allows for shorter observation periods and prevents loss of relative accuracy as a result of mapping errors into a global reference frame. The velocities with respect to the reference station are estimated as a linear fit through the time series of their relative positions. Daily network comparisons show small, randomly distributed residuals at each station and no systematic network rotation is found. The RMS of the daily coordinate repeatabilities with this technique is 2, 2 and 8 mm for each direction between 1998 and 2004, with slightly higher values in 1997 when some transect sites were occupied for only 3 to 4 hours. Long-term uncertainties (epoch residuals relative to a linear trend) have the same amplitude (a few mm) as the short-term uncertainties (daily repeatabilities). This agreement indicates that uncertainties are correctly estimated and that station positions are free of unidentified biases. Hence the Palu transect relative processing, although based on both fewer and shorter observation periods, delivers (relative) velocity estimates with an uncertainty (1σ) ranging from

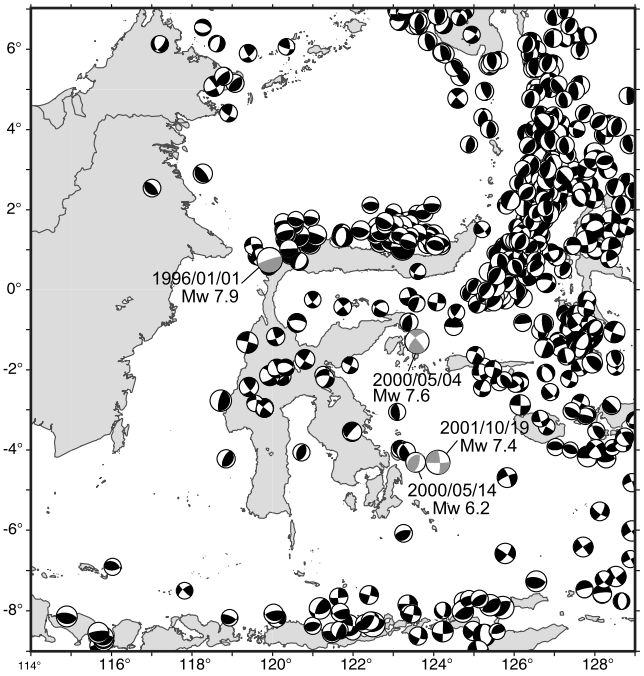

Figure 3. Post-1976 instrumental CMT focal mechanisms from Harvard catalogue in the Sulawesi area. The size of the symbol is proportional to the earthquake magnitude. Focal mechanisms in grey, labeled by date (year/month/day) and magnitude, correspond to the earthquakes cited in the text.

0.3 to 1.5 mm/yr for the sites that were measured at least 3 times.

3.3. Obtaining a Consistent Velocity Field

[11] The Palu transect velocities are processed relative to the westernmost station of the transect, WATA. In order to get the velocities of the transect in a global reference frame, we simply add the velocity of WATA in ITRF-2000 to all the points of the transect. In doing this we assume that the transect is affected only by translation at such a small scale (60 km at most). Indeed, the two independent determinations (relative and regional) of the velocity of the transect's easternmost site (TOBO, also continuously measured) with respect to that of WATA agree within 0.6 mm/yr. The velocities (in the ITRF2000) of this combined solution (regional + relative) are listed in the auxiliary material.[1]

4. Modeling the Velocity Field

4.1. Description of the Velocities in Sulawesi Area

[12] We specify several tectonic blocks in the Sulawesi region based on the GPS velocities and the geological and seismological evidence for active faulting. Figure 2 displays the velocities relative to the Sunda Plate reference frame [*Socquet et al.*, 2006; Simons et al., unpublished manuscript, 2005], and Figure 3 shows the focal mechanisms in the same region. The first obvious pattern from the GPS velocities is the division of the island into two independent domains. In the south, the Makassar Block (grey arrows) displays a small but significant motion relative to Sunda appearing to rotate anticlockwise around a pole located near its southwestern tip. The Makassar Trench (Figure 4) bounds this block to the west and accommodates at least part of the Sunda/Makassar convergence. The East Sulawesi Trench constitutes the boundary of the Makassar and East Sula blocks with the Banda Sea. The northern half of Sulawesi (black arrows) moves toward the NNW and rotates clockwise around a pole located near its northeastern tip. The northern half of Sulawesi is divided into three smaller blocks. The eastern part of the northern arm of Sulawesi, here named the Manado Block, has an independent motion from the North Sula Block. These two entities are separated by the Gorontalo Fault, evident in geology. The boundary between the Makassar and North Sula blocks is the Palu-Koro Fault. Last, the eastern arm of Sulawesi also shows independent motion from North Sula, indicated by west trending GPS vectors at sites LUWU, AMPA, and KAMB. Because of the sparseness of our network in this area, more exact boundaries of this block (here named East Sulawesi) are difficult to draw. East of Sulawesi, we define the Banda Sea as a rigid block on which we have only two GPS velocities: at SANA and AMBO.

4.2. Data Modeling Approach

[13] The relatively small, rotating blocks are surrounded by active faults where interseismic coupling produces elastic deformation within the blocks. In many instances, a substantial amount of the block's surface is below sea level and inaccessible to standard GPS measurements so only a part of the block has constraints. For example, in the northern half of Sulawesi the Tomini Gulf covers the central

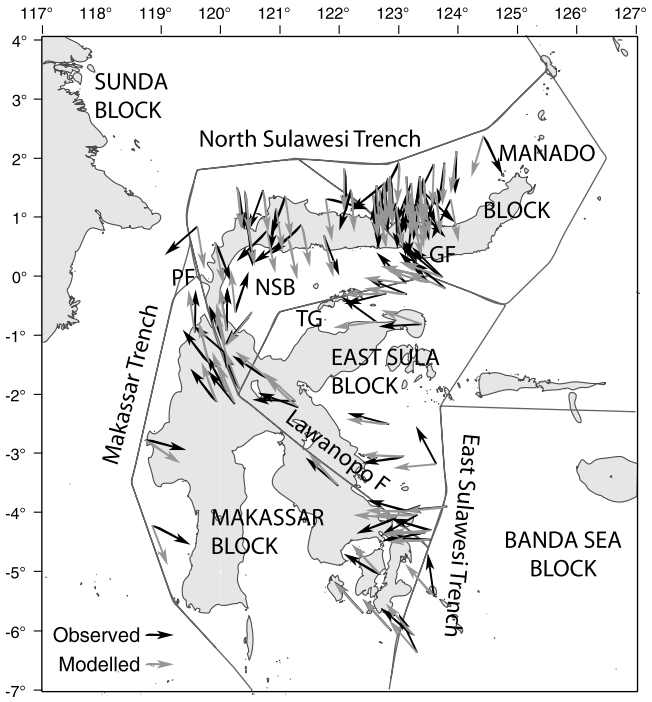

Figure 4. Blocks geometries used for the modeling. The observed (black) and the modeled (grey) slip vectors of model 2 are also shown. NSB, North Sula Block; PF, Palu Fault; TG, Tomini Gulf fault zone; GF, Gorontalo Fault.

[1]Auxiliary materials are available at ftp://ftp.agu.org/apend/jb/2005jb003963.

Table 1. Probablilities Derived From *F* Tests of Block Independence for Various Tectonic Blocks/Faults Models[a]

Model	Number of Blocks	Number of Data	Number of Parameters	DOF	χ^2_n	Is Model 2 Better?	
						Probability, %	Answer
1, GPS only	6	100	22	78	8.3	91	yes
2, GPS plus SV, best model	6	191	27	164	6.4		
3, MANA = NSUL	5	191	23	168	6.6	56	maybe
4, NSUL = ESUL	5	179	23	156	7.2	76	maybe
5, ESUL = MANA	5	191	24	167	8.2	94	yes
6, ESUL = NSUL = MANA	4	179	19	160	7.4	80	yes
7, MAKA = ESUL	5	187	24	163	12.3	99	yes
8, BSEA = MAKA	5	185	24	161	10.8	99	yes

[a]Except for model 1 where only GPS data were used, all GPS and slip vector (SV) data were used for these models. In model 1, the coupling ratio along all the faults was uniform. In the other models, the coupling ratio is allowed to vary along the Palu Fault and the Minahassa–North Sulawesi Trench and is uniform along the other faults. Models 3 to 8 are derived from model 2, with fewer blocks considered. For each model, the blocks listed comprise a single rotating unit. DOF, degree of freedom; χ^2_n, normalized chi-square.

part of the area (Figure 2). Because of the limited sampling, it is difficult to identify observation points that may indicate rigid block rotations only, i.e., no closer than 100km from any active fault. Consequently, the velocities of most points result from a combination of rigid rotations and elastic loading on faults. Therefore we use an inversion approach that simultaneously estimates the angular velocities of elastic blocks on a sphere and creep fractions (e.g., coupling coefficients) on block-bounding faults. For this purpose we use the DEFNODE software [*McCaffrey*, 1995, 2002, 2005] which applies simulated annealing to downhill simplex minimization [e.g., *Press et al.*, 1989] to solve for the model parameters. We minimize data misfit, defined by the reduced chi-square statistic: $\chi^2_n = (\sum r^2/s^2)/\mathrm{DOF}$, where r is the residual, s is the standard deviation and DOF gives the degrees of freedom (number of data minus number of free parameters).

[14] The coupling fraction (ratio of locked to total slip) on the fault is defined as a purely kinematic quantity, φ. If $\varphi = 0$, the fault is creeping at the full long-term slip rate and if $\varphi = 1$, the fault interface is fully locked during the interseismic period. Since the GPS data we use are sparse, we assume that this coupling fraction is uniform over large patches of the faults. However, we allowed it to vary along the Palu Fault and the Minahassa Trench in some inversions where the GPS arrays are denser. The relative motion on the faults is determined by the Euler vectors describing the motions of the blocks adjacent to the fault. The slip rate deficit vector on the fault is the scalar coupling value φ multiplied by the relative motion vector between the two blocks at a given fault. The elastic contribution to the velocity field from the fault slip rate deficit is calculated using a back slip approach to elastic dislocation modeling [*Savage*, 1983], using the formulations of *Okada* [1985] for surface displacements due to dislocations in an elastic half-space.

4.3. Results of the Models

[15] In the first model presented here, we use GPS data only (applying the 2-sigma uncertainty) to estimate the angular velocities of five blocks (North Sula, Makassar, Manado, Banda Sea, East Sula) and the average coupling ratio on seven faults bounding the blocks (Palu Fault, Gorontalo Fault, Minahassa Trench, Makassar Trench, East Sulawesi Trench, Lawanopo Fault, and Tomini Gulf fault zone, Figure 3). Given the high number of sites located near the Palu and Gorontalo faults compared to the number of sites located on the stable blocks away from faults, we down weigh the former by a factor of 4 to estimate the blocks rotations using the geographically distributed data. We obtain $\chi^2_n = 8.3$ (100 observations, 78 degrees of freedom, Table 1). This model produces very large uncertainties in the estimates of some block motions and fault coupling coefficients (on the east Sulawesi Trench, for example, Table 2). Therefore, in a second inversion, in addition to the GPS data, we use earthquake slip vector azimuths extracted from Harvard centroid moment tensor (CMT) focal mechanisms (Figures 3 and 4). We apply an uncertainty of 10° on the azimuth of the slip vectors except for those from the Minahassa Trench, where the uncertainty has been fixed at 20° for the western part and 40° for the eastern part because of the abundance of earthquake data in these areas. In this model, we allow the coupling ratio of the Palu Fault and the Minahassa Trench to vary along strike. Although we have in this second model more parameters to estimate, the addition of these slip vector data reduces χ^2_n to 6.4 (191 observations, 164 degrees of freedom) and reduces uncertainties on the blocks' Euler vectors by a factor of 2 to 3. The χ^2_n obtained for the best model decreases to 3.6 if the outliers (AMBO and WUAS) are excluded from the model. The misfit to the data remains however high, indicating that the formal uncertainties derived from the GPS processing are underevaluated and still poorly estimated. For the present data set, to obtain a realistic estimate of the error on the GPS velocities, one should take 4-sigma of the formal uncertainty given in Table S1 in the auxiliary material (in the inversion, uncertainties have already been scaled by 2).

[16] Table 3 summarizes the poles of rotation we obtain for the various blocks and models. It is noticeable that the poles obtained by the two inversions are similar for the blocks that have several GPS velocities (i.e., North Sula, Manado and Makassar blocks). However, slip vectors provide useful constraints for the blocks that have sparse GPS observations (East Sulawesi Block and Banda Sea Block). Table 2 gives the fault geometries at depth, the estimated coupling ratios and slip rates for the two models. Once again, the estimation of the coupling ratio is improved by the addition of slip vector constraints for the faults that are not surrounded by GPS stations (Makassar Trench, East Sulawesi Trench, Lawanopo Fault and Tomini Gulf fault zone). However, the amount of coupling on the Palu Fault, the Gorontalo Fault and the Minahassa Trench is better determined in the model with GPS data only, since the local networks around these faults are very dense. Also note that

Table 2. Summary of Fault Parameters[a]

Fault	Dip	Depth, km	φ	$\Delta\varphi$	Slip Rate, mm/yr	Azimuth, deg
			Model 1, GPS Only			
Palu	50°	12	1	0.06	41/45	−20/7
Gorontalo	80°	10	1	0.70	11/12	−7/0
Minahassa Trench (west)	20–30°	50	0	0.15	42/50	−3/−3
Minahassa Trench (east)	20–30°	50	0	0.15	13/23	15/−1
Makassar Trench	25–35°	20	1	0.54	4/13	−42/−67
East Sulawesi Trench	20–30°	20	1	1.40	9/19	−74/−32
Lawanopo	50°	15	1	0.39	25/26	−59/−43
Tomini	50°	15	1	0.69	28/18	−52/−142
			Model 2, GPS and Slip Vectors			
Palu	50°	12	1/1	0.16/0.91	41/44	−21/7
Gorontalo	80°	10	1	0.85	11/12	−14/−6
Minahassa Trench (west)	20–30°	50	0/0	0.3/0.54	41/49	−3/−4
Minahassa Trench (east)	20–30°	50	0/0	7.23/29.34	13/23	20/2
Makassar Trench	25–35°	20	1	0.50	5/11	−49/−68
East Sulawesi Trench	20–30°	20	0.64	0.43	2/27	−97/−43
Lawanopo	50°	15	1	0.36	23/24	−51/−36
Tomini	50°	15	1	0.79	23/25	−44/−151

[a]Dip and depth represent the dip angle and maximum locking depth for the faults; φ and $\Delta\varphi$ represent the coupling ratio and 1-sigma uncertainty. In model 1 (only GPS data used) the coupling ratio was assumed to be uniform along all faults while in model 2 (GPS and slip vectors used) the coupling ratio is allowed to change along the Minahassa Trench and the Palu Fault. Since slip rate and slip azimuth vary along the faults, we give the range of these values.

the locking depth of the Gorontalo and Palu faults are well constrained by the width of the arctangent evident in the horizontal displacement profile of the GPS transect, while it has been fixed a priori for the other faults.

5. Discussion

5.1. Makassar Block

[17] The residual velocities of the sites on the Makassar Block are mainly below 3 mm/yr and display no systematic orientation, suggesting that it deforms little internally. With respect to Sunda, the Makassar Block rotates anticlockwise around a pole located near its southwestern tip (Table 2 and Figure 5). Because of this rotation, convergence on the Makassar Trench increases northward with a corresponding increase in slip rate deficit (Figure 6). Deformation associated with this margin may also extend into eastern Kalimantan. Stations on the eastern margin of Borneo (SAND, TAWA, TNJB, BLKP) display residual velocities of up to 7 mm/yr with respect to the Sunda Plate (Figure 2). Westward motion of ~5mm/yr at the equator latitude (TNJB station, 1° north) decreases to 1–2 mm/yr at both the northern and southern ends of the island (stations of SAND at 6° north, BLKP and BATU at 1° and 4° south) implying a clockwise rotation of the eastern margin of Borneo north of the equator and an anticlockwise rotation south of it. This deformation may be distributed and cannot be described in terms of rotation of rigid blocks. It might be explained by initiation of a collision in the Makassar Strait between the eastern Borneo shelf and the westward moving Makassar and North Sula blocks.

Table 3. Euler Vectors Used in This Study[a]

	Euler Vector					
Plates Pairs	Longitude deg	Latitude, deg	ω, °/Myr	Emax, deg	Emin, deg	Azimuth, deg
Sunda/ITRF2000[b]	−48.9	85.8	−0.3			
			Model 1, GPS Only			
Makassar/Sunda	−4.5	117.4	1.5 ± 0.21	0.48	0.26	83 ± 3
North Sula/Sunda	2.4	129.9	−2.5 ± 0.36	2.23	0.17	193 ± 9
Manado/Sunda	1.9	126.6	−3.1 ± 0.99	1.06	0.49	251 ± 3
Banda Sea/Sunda	−7.1	118.1	2.0 ± 0.91	6.92	1.30	70 ± 10
East Sula/Sunda	−8.3	115.7	2.4 ± 1.31	7.35	0.85	43 ± 9
			Model 2, GPS and Slip Vectors			
Makassar/Sunda	−4.8	117.4	1.4 ± 0.15	0.42	0.21	71 ± 3
North Sula/Sunda	2.4	129.5	−2.6 ± 0.38	1.81	0.32	247 ± 8
Manado/Sunda	1.8	126.5	−3.2 ± 1.99	1.44	0.37	262 ± 3
Banda Sea/Sunda	−9.7	113.3	1.8 ± 0.21	2.55	0.63	54 ± 15
East Sula/Sunda	−7.9	115.0	2.2 ± 0.55	3.70	0.50	48 ± 9

[a]The parameter ω is the rotation rate with one standard error. Euler vectors are for the first plate relative to the second one. Emax, Emin, and azimuth refer to the maximum and minimum axes of the 68% confidence error ellipse and the azimuth of the major axis, respectively. Positive rotation rates indicate anticlockwise motion looking from above.
[b]From Simons et al. (unpublished manuscript, 2005).

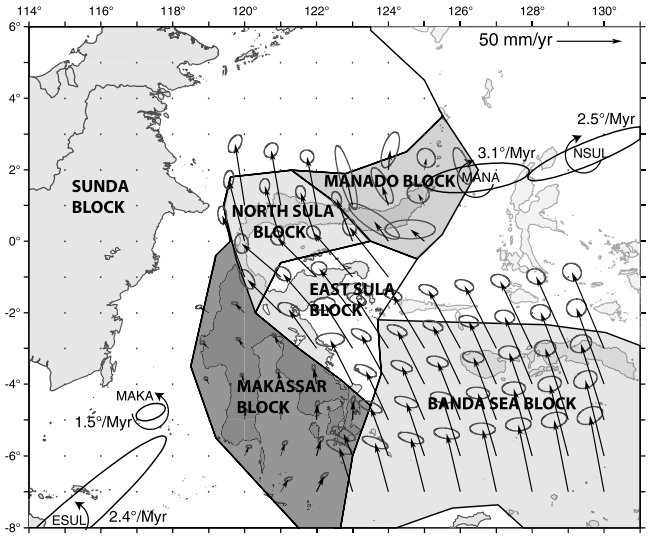

Figure 5. Rotational part of the inferred velocity field in the Sulawesi area (relative to the Sunda Plate) as predicted by the Euler vectors of the best fit model (model 2). Error ellipses of predicted vectors show the 99% level of confidence. Also shown are poles of rotation and error ellipses (with respect to the Sunda Plate) from the best fit model. Curved arrows indicate the sense of rotation, and numbers indicate the rotation rate. MAKA, Makassar Block; MANA, Manado Block; ESUL, East Sula Block; NSUL, North Sula Block.

[18] On the eastern southside of Sulawesi, the East Sulawesi Trench is also active. Two large earthquakes occurred there: 14 May 2000 M_w 6.2 and 19 October 2001 M_w 7.4 (Figure 3). Sites BAUB and KEND are located within the elastic deformation zone associated with the trench indicated by significant displacements detected in their time series at the epoch of the earthquakes. Hence we use only the epochs before these events (1994–1998, auxiliary material) to determine the long-term interseismic velocities of the two sites. The two velocities and slip vector data are matched by a slip deficit of 15 mm/yr accommodated on a plane striking north and dipping at 20–30° fully locked down to 20 km depth (Figures 4 and 6).

5.2. North Sula Block

[19] Uncertainties on the Euler vector for the North Sula Block are high in the NE direction because the GPS data are spread in a line because of the shape of the north end of the island (Figure 2). In addition, many sites have been affected by earthquakes (Figures 2 and 3). Their time series are not linear but instead show logarithmic postseismic decay trends making their interseismic velocities difficult to determine. All sites near the Minahassa Trench (north side of the block) were displaced by the 1 January 1996 M_w 7.9 earthquake (Figure 3) leaving few sites on the stable part of the block (SGTI, PALA, and GT03). Other sites on the block are within the strain areas of the Palu-Koro and Gorontalo faults. In the southern part of the block, the large residual velocity of site WUAS (Figure 6) probably arises because the site is within a complex and poorly modeled junction of three block-bounding faults. A connection of the Palu Fault to the Matano Fault instead of to the Lawanopo Fault may improve this fit but in this area the exact location of the fault is poorly known.

[20] Using GPS velocities, slip vectors and a joint inversion for block rotation and fault coupling we obtain a North Sula – Sunda pole near 2.4°N and 129.5°E rotating clockwise at 2.6°/Myr (Table 3). This pole is 3–4° east of and slower than the poles estimated by previous GPS and geologic studies [*Stevens et al.*, 1999; *Walpersdorf et al.*, 1998b; *Silver et al.*, 1983a]. We conclude that the North Sula region comprises a rapidly rotating microblock pinched between strike-slip faults (Palu, Lawanopo, and/or Matano) and subduction, revealing accumulation of both interseismic elastic strain and internal deformation (Figure 6).

5.3. East Sulawesi Block

[21] The sites AMPA and LUWU show significant, large motions trending west relative to the North Sula Block and are not compatible with rotating with either the North Sula or Manado Block. Accordingly, we introduce another independent block, the East Sula Block, though the boundaries are not well defined. To the south, we bound it along the Lawanopo Fault (Figure 4) which displays moderate seismicity. However, the Matano Fault, located north of the Lawanopo, is also active. Hence the deformation is poorly represented in the region between the Matano and Lawanopo faults. The northern boundary is taken as the roughly E-W zone of frequent seismicity beneath the Tomini Gulf (Figure 3).

[22] Since only three GPS velocities are available for the East Sulawesi Block, slip vectors from earthquakes located on its boundaries provide important constraints on its motion. The Euler vector that we obtain is near 7.9°S, 115.0°E (with an anticlockwise rotation rate of 2.2°/Myr) with respect to Sunda (Table 3), leading to ~25 mm/yr of left-lateral strike slip on the Lawanopo Fault and ~24 mm/yr of right lateral motion along the Tomini Gulf boundary. Inversions were run to test the independence of the East Sulawesi Block from the North Sula and Makassar blocks. F tests suggest that the East Sulawesi Block is disconnected at 99% confidence from the Makassar Block and at 76% confidence from the North Sula Block (Table 1).

5.4. Manado Block and Gorontalo Fault

[23] In the North Sula Block reference frame, the sites located at the eastern termination of the northern arm of Sulawesi display residual velocities ranging from 8 to 11 mm/yr and hence belong to a different block. The Gorontalo Fault, which bisects the northern arm of the island, is taken as the boundary between the Manado Block and the North Sula Block. Our best fit pole for the Manado Block is near 1.8°N, 126.5°E with an anticlockwise rotation rate of 3.2°/Myr (Table 3). The velocity residuals are mostly less than 2 mm/yr (Figure 6, bottom right). The computed Manado/North Sula relative Euler vector predicts 11 mm/yr of right-lateral slip across the Gorontalo Fault. Our velocity profile shows an accumulation of interseismic elastic deformation across this fault locked to about 10 km depth (Figure 7).

[24] F tests show that the Manado Block is independent from the North Sula Block (56% confidence, Table 1) and

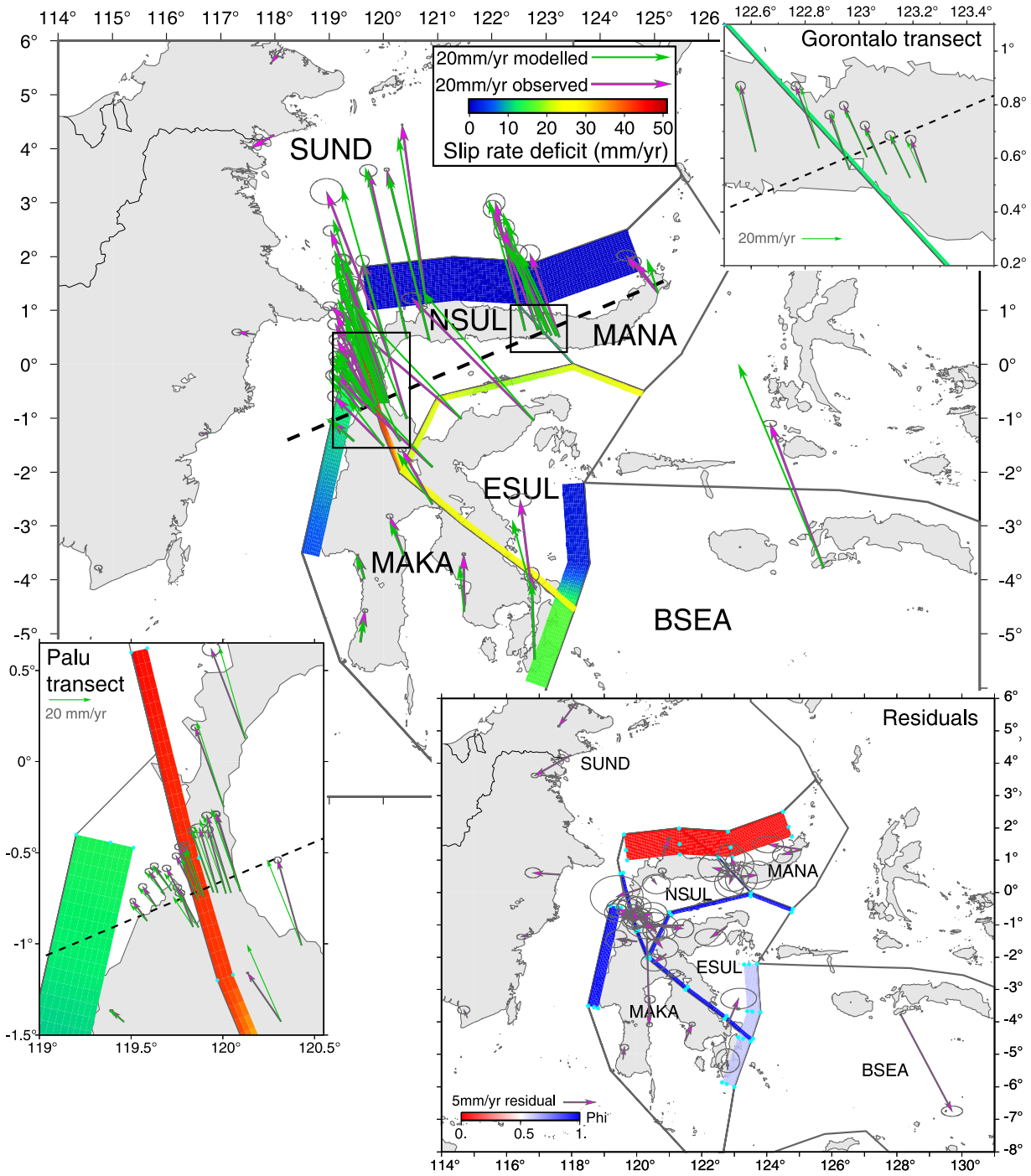

Figure 6. Best fit block model derived from both GPS and earthquakes slip vector azimuth data. Center: Observed (red) and calculated (green) velocities with respect to the Sunda Block (shown are 20% confidence ellipses, after GPS reweighting; see text). The slip rate deficit (mm/yr) for the faults included in the model is represented by a color bar. The profile of Figure 7 is located by the dashed black line. The black rectangles around Palu and Gorontalo faults localize the insets. Top right and bottom left insets show details of the measured and modeled velocities across the Gorontalo and Palu faults. The bottom right inset shows residual GPS velocities with respect to the model. The value of the coupling ratio, φ, for the faults included in the model is represented by the color bar. Light blue dots represent the locations of the fault nodes where the coupling ratio is estimated. Nodes along the block boundaries are at the surface of the Earth, and the others are at depth along the fault plane. In this model, φ is considered uniform along strike and depth for all the faults, except for Palu Fault and Minahassa Trench, where it is allowed to vary along strike.

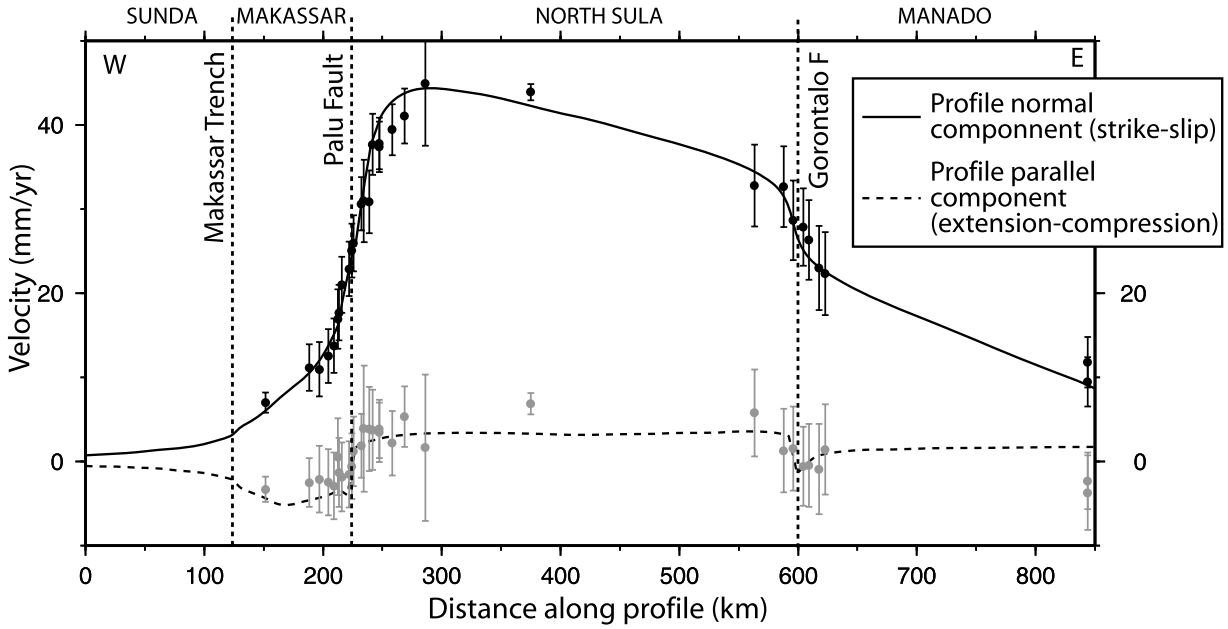

Figure 7. Velocity profile across Makassar Trench, Palu Fault, and Gorontalo Fault (profile location in Figure 6) in Sunda reference frame. Observed GPS velocities are depicted by dots with 1-sigma uncertainty bars, while the predicted velocities are shown as curves. The profile normal component (approximately NNW) (i.e., the strike-slip component across the NW trending faults) is shown with black dots and solid line, while the profile-parallel component (normal or thrust component across the fault) is shown with grey dots and a dashed line. Where the profile crosses the faults and blocks is labeled.

the East Sula Block (94% confidence). Although the *F* test does not completely reject the possibility of Manado and North Sula blocks being a single block, the gradient in the velocities across the Gorontalo Fault appears to be too large to be due to rotation of a single block, arguing the North Sula Block and the Manado Block are two different entities.

5.5. Minahassa Trench

[25] Very interestingly, we find no elastic deformation associated with locking on the Minhassa subduction fault (Figure 6 and Table 2). While the lack of coupling is well determined for the western Minahassa Trench due to the proximity of several GPS sites, it is poorly determined for the eastern part (Table 2) because GPS sites are sparse there. In the alternative models 5 and 6, where the North Sula and Manado blocks move as one, coupling on Minahassa Trench varies along strike perhaps compensating for the lack in rotation of the Manado Block. In this case, the trench appears to be locked at its eastern part, but remains poorly locked on its western part.

[26] The null locking observed in the western part cannot represent its long-term behavior since it produced a magnitude 7.9 earthquake in January 1996 (Figure 3) that produced significant coseismic ground displacements [*Gómez et al.*, 2000]. The GPS velocities above the western end of the trench are still affected by postseismic deformation from that earthquake, which may be causing the low coupling estimate The present-day low coupling is representative of a postseismic temporary stage during which the interseismic elastic deformation away from the trench is compensated by postseismic deformation (motion toward the trench), similar to what has been observed on the Japan Trench following the 1994 Sanriku-Oki M_w = 7.6 earthquake [*Mazzotti et al.*, 2000]. Presumably, full locking and accumulation of elastic strain will resume following the postseismic deformation.

5.6. Palu Fault Interseismic Deformation

[27] The computed North Sula/Makassar Euler vector predicts a slip rate of 41 to 44 mm/yr with an azimuth rotating from 21°W to 7°E, from south to north, on the Palu-Koro fault zone. For accessibility reasons, the GPS profile was installed in the vicinity of Palu city, where the fault appears to be a pull-apart structure in the morphology [*Beaudouin et al.*, 2003; *Bellier et al.*, 2001, 2006].

[28] We present two plausible models of the deformation in the pull-apart area. The first model is derived from the inversion for the regional Sulawesi kinematics and involves a single fault locked at depth, while the second model involves several parallel, shallowly locked faults.

[29] The velocities measured across the transect fits a single dislocation model of the fault interseismically locked to a depth of 12 km, consistent with the previous studies [*Stevens et al.*, 1999; *Walpersdorf et al.*, 1998c]. In the current study however, the fault appears to be dipping at 50° toward the east, accommodating ~11–14 mm/yr of extension, in addition to 39 mm/yr of strike slip (bottom left inset in Figure 6 and Figure 7 and Table 2). The normal component of faulting in the region of Palu inferred from the geodetic data is in agreement with triangular facets, indicating an active normal motion, observed in the morphology [*Beaudouin et al.*, 2003; *Bellier et al.*, 2001, 2006].

[30] In the alternate model, we use several parallel dislocations to explain the pull-apart geometry (Figure 8, top). The GPS data are fit best by a model of four parallel left-lateral strike-slip dislocations (Figure 8, bottom).

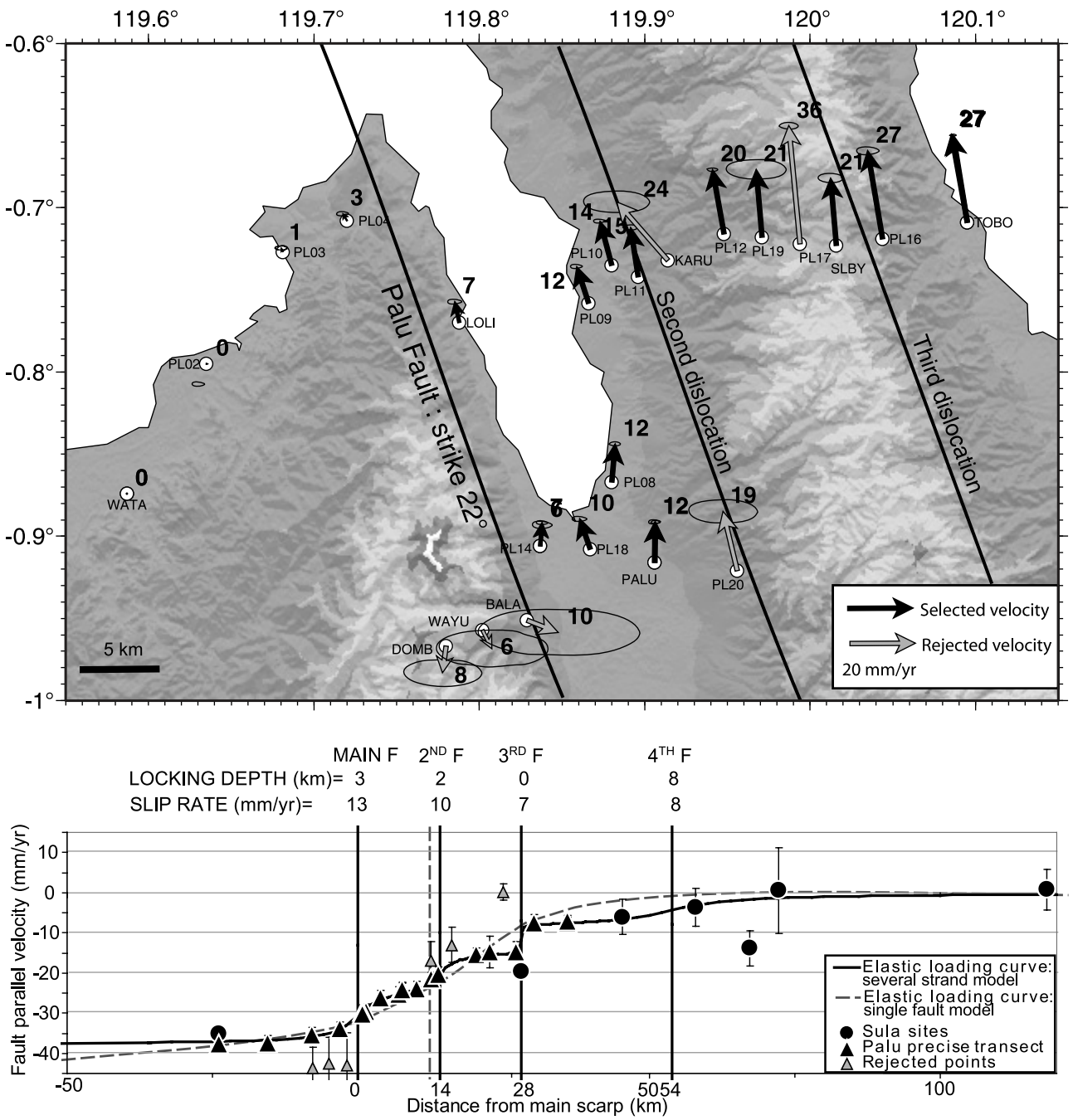

Figure 8. (top) GPS velocities in Palu area relative to station WATA. STRM topography is used as background. (bottom) Four parallel elastic dislocations that fit best the velocities in the Palu fault zone. The fault-parallel component of the GPS velocities (with 1-sigma error bars) is plotted with respect to their distance to the main fault scarp, in the North Sula Block reference frame. The black curve represents the fault-parallel modeled velocity of the four strand model. For comparison, the fault-parallel modeled velocity predicted by the single fault model is also plotted (grey dashed curve). The location of the modeled dislocation is represented as vertical bars for each model (black and dashed grey lines, respectively).

[31] 1. The first dislocation is located along the western side of the pull-apart, recognized by geologists as being the active Palu Fault scarp [*Beaudouin et al.*, 2003; *Bellier et al.*, 2001, 2006]. It accommodates 13 mm/yr, and its locking is between 2 and 5 km depth (Figure 6).

[32] 2. The second dislocation is 14 km east of this main scarp, accommodates 10 mm/yr and is locked between 1 and 5 km depth. This second dislocation, located along the eastern coast of the Palu Gulf, corresponds to the fault that bounds the Palu pull-apart to the east. It separates Mio-Quaternary molasses from the metamorphic bedrock [*Bellier*

et al., 2006] and has been activated during the February 2005 $M_w = 6.3$ earthquake (A. Soehaimi et al., personal communication, 2006).

[33] 3. The third dislocation is located 28 km from the main scarp and accommodates 7 mm/yr. Its locking depth tends to zero, which is equivalent to a creeping behavior. The dislocation is near a steep gradient in topography that could correspond to a fault scarp. The abruptness of the step in the velocities depends on the velocity determination of the sites SLBY and PL16 (measured 3 and 4 times, respectively).

[34] 4. The three previous dislocations accommodate 30 mm/yr of the relative block motion. Another 8 mm/yr are missing and seem to be accommodated over a broad zone 50 km to the east. Dense GPS measurements are missing to discriminate whether these 8 mm/yr are localized on one single dislocation or are distributed. Velocities are fit well by including a fourth dislocation locked at 5–15 km depth and located ~54 km east of the main scarp. The parameters of this last dislocation are poorly constrained by three sites (DONG, SGTI, PALA) that are well to the north of Palu and span 1° in latitude.

[35] The GPS inferred strike-slip rate (39 mm/yr) for the Palu Fault agrees with the long-term slip rate (35 ± 8 mm/yr) determined from stream and fan offsets, mainly seen in the quaternary deposits along the western border of the Palu basin [*Bellier et al.*, 2001]. This long-term slip rate, ranging from 5 to 51 mm/yr [*Bellier et al.*, 2001], argues for the single dislocation model at its high end, although the alternate local model, that predicts 13 mm/yr on the western branch of the fault, is also within the long-term range. South of the Palu basin, where the fault trace is more linear and appears to form a single trace, *Bellier et al.* [2001] obtain a slip rate of 29 ± 5 mm/yr. This rate might either correspond to the "single strand model" or to the 30 mm/yr (13 + 10 + 7) of total amount taken on the three western dislocations of the "multiple strand model."

[36] In terms of seismicity, preliminary paleoseismological studies reveal three $6.8 < M_w < 8$ earthquakes over the last 2000 years [*Bellier et al.*, 2001], implying a cumulative offset of ~30 meters [*Wells and Coppersmith*, 1994]. These earthquakes occurred on the main branch of the fault, western side of the pull-apart. The measured cumulative offset matches quite well the 26 meters of cumulative offset predicted by the multiple strand model on the western dislocation. Low slip on the western strand reconciles the fact that although the paleoseismicity is small, the fault is interseismically locked and releases its strain through earthquakes. If the multiple strands model is accurate, additional paleoseismic studies on the secondary branches of the Palu Fault should be performed to sample more completely the paleoseismicity, and hence assess the complete seismic hazard of the fault zone. However, because paleoseismological studies are able to detect only the larger earthquake events ($M_w \sim 6.5$ and above), there may be other smaller ones contributing to a slip rate. Paleoseismology is most likely slightly underestimating the rate. It is also possible that there could be periodic aseismic slip on this fault (postseismic, or episodic slow slip?), so the paleoseismology underestimates the slip rates even more if those occur. If that is the case, the single Palu Fault model might be more accurate (rather than the three to four strands). However, small earthquakes ($M_w < 6$) should be numerous to contribute significantly to a slip rate (one every 1 or 2 years on the 150 km long Palu segment), which is not observed in the instrumental seismicity. Strong geomorphic evidence of a pull-apart in this area combined with the recent seismic activity of the east branch of the pull-apart pleads for the multiple strand model. Therefore we consider that the "one-dislocation" model is a good large-scale approximation (good enough when dealing with block rotations over a long period of time for example) but that a refined model with more dislocations is needed by geodetic, geomorphic and seismologic data when dealing with local fault behavior and assessing the seismic hazard. These scenarios are not equally probable, they happen at the same time: in this area, a transtensive motion occurs on the fault system, which is probably divided into several active branches (each side of the pull-apart), that may be regarded as surface splays of a strike-slip flower structure.

6. Conclusion and Outlooks

6.1. Kinematics of the Triple Junction and Possible Mechanisms Driving the Microblock Rotations

[37] Sulawesi is located at the western termination of the boundary between Australia and Philippine/Pacific plates. This boundary accommodates the left lateral oblique convergence by rapid microblocks rotations in Papua New Guinea [*Bock et al.*, 2003; *Pubellier and Ego*, 2002; *Pubellier et al.*, 1996; *McCaffrey and Abers*, 1991; *Stevens et al.*, 2002; *Wallace et al.*, 2004] and slip partitioning further west (between normal subduction at the Timor Trough and strike slip on the Sula-Sorong Fault, Figure 1). Movements of crustal fragments within this E-W oriented complex boundary zone results in local collisions with the Sunda Plate in the area of Sulawesi and Borneo. Because of the rapid westward motion of the Philippine Sea Plate, the Sula-Sorong Fault slips left laterally. It ends in Sulawesi (there called Matano/Palu-Koro Fault), where it separates the island in two parts. The southern blocks of the study area (Makassar, Banda Sea and East Sula blocks, Figure 5) rotate anticlockwise, which is consistent with a left lateral sense of shear. The northern parts of Sulawesi however (North Sula and Manado blocks) rotate clockwise: the North Sula Block rotates quickly, while the Manado Block is swept along the latter and rotates at a slower rate (relative to the fixed Sunda Block).

[38] We suggest that the clockwise tectonic block rotation in the northern part of Sulawesi occurs due to the change in boundary condition around the North Sula Block. To the west the Sulawesi Island is bound by buoyant Borneo continental crust, while oceanic crust bounds the island to the north (Celebes Sea) and to the east (Banda Sea). Because of its thick, buoyant crust, the Borneo lithosphere resists subduction below Sulawesi. Such buoyancy forces have been termed "colliding resistance" forces [*Forsyth and Uyeda*, 1975]. This collision inhibits rapid convergence between Borneo and Sulawesi but results in slow deformation of the eastern margin of Borneo island. Conversely, the presence of oceanic crust north and east of Sulawesi facilitates subduction. North of Sulawesi at the Makassar Trench, "trench suction" forces [*Elsasser*, 1971; *Forsyth and Uyeda*, 1975; *Chapple and Tullis*, 1977; *Chase*, 1978]

allow the extrusion of material toward the north. The westward motion of the northern part of Sulawesi is hence more easily accommodated by a clockwise rotation of the North Sula Block than by mountain building, since a relatively low stress boundary exists toward the north. The same kind of process has been invoked in other places (e.g., westward extrusion of the Bird's Head Block in western Papua [*Pubellier and Ego*, 2002; *McCaffrey and Abers*, 1991; *Stevens et al.*, 2002] or extrusion models for the deformation of Asia in response to the Indian indenter [e.g., *Tapponnier et al.*, 1982]). Similarly, the decrease of the motion from the Banda Sea Block to the Makassar Block might not only be due to a westward decreasing left-lateral shear but also to collision of the Makassar Block with Borneo continental crust. These ''colliding resistance'' forces would cause the E-W convergence to be instead accommodated on the East Sulawesi Trench, where the Banda Sea oceanic crust can easily subduct under the Makassar Block's continental lithosphere.

6.2. Interseismic Behavior of Faults

[39] The Sulawesi microblocks are surrounded by active faults that produce elastic deformation inside them. We monitored two active strike-slip faults in the region of Sulawesi using two dense local GPS networks. The Gorontalo Fault appears to be active although little seismicity is evident in this area. The fault accommodates 11 mm/yr in dextral transtension and is locked to about 10 km depth. The Palu Koro Fault zone accommodates 42 mm/yr and shows a transtensive behavior more complex than the simple strike slip commonly described (39 mm/yr of left-lateral strike slip associated with $\sim$11–14 mm/yr of extension). This deformation is most likely explained by the presence of a pull-apart structure that may be localized around the Palu area. We present here two models that can explain the deformation in this area. The first model is a good large-scale approximation and involves one single transtensive fault, while the second involves three closely spaced ($\sim$14 km apart) faults with shallow locking depths accommodating a total amount of 30 mm/yr, the remaining motion being accommodated 50 km to the east. That refined three dislocation model has important consequences concerning the seismic hazard: the coexistence of three dislocations with very shallow locking depths may explain the deficit of paleoseismicity on the one studied surface trace of the fault. The GPS inferred slip rate agrees with the long-term slip rate determined from stream and fan offsets [*Bellier et al.*, 2001]. The Lawanopo/Matano Fault zone, extending from the Palu Fault toward the south, is probably coupled in the interseismic period. It is still poorly known which of these faults is the southern continuation of the Palu Fault. Sulawesi is surrounded by three active trenches. The East Sulawesi Trench accommodates the motion between the Banda Sea and the Makassar Block. This trench is affected by periodic earthquakes between which strain is accumulated above the locked subduction plane. To explain our measured velocities properly, another locked fault must be located in the Makassar Strait. Finally, the Minahassa Trench bounds the island to the north and accommodates the motion of the North Sula Block relative to the Sunda Plate. We find here a null coupling for this trench that has generated very large subduction earthquakes in the recent past [*Gómez et al.*, 2000]. Hence this absence of loading cannot represent the regular interseismic behavior of the trench and is certainly a transient state maybe due to afterslip following a recent seismic event [*Mazzotti et al.*, 2000].

6.3. Limitations of the Model

[40] To fully represent the interseismic deformation, the time series of the sites affected by earthquakes should be analyzed in terms of transient displacements, coseismic jumps and postseismic deformation. Beyond its crucial interest for a better understanding of the earthquake cycle, such modeling can also allow better determination of the interseismic velocity required for kinematic studies. However, constraining coseismic and postseismic deformation requires long and dense (temporally and spatially) time series (ideally, those provided by permanent GPS stations) that are still missing at most sites.

[41] The current model explains the data and describes the kinematics and the behavior of the active structures around Sulawesi. Given the sparseness of the data, the interseismic coupling on several of the faults should only be taken as a first approximation. However, the deformation around Palu and Gorontalo faults is accurately modeled. Our detailed analysis in the Palu area revealed several subsurface splays of the fault unknown prior to this study.

[42] **Acknowledgments.** This work is a continuation of the joint research activities in SE Asia, which were initiated by the GEODYSSEA project. Thanks and appreciation are extended to all people who have contributed significantly in expanding the GPS database on SE Asia. We would like to thank especially all the staff and students at the Geodesy department of the Institut Teknologi Bandung and the Geodynamics division of the National Coordination Agency for Surveys and Mapping (BAKOSURTANAL) in Indonesia for their contribution to the GPS measurements in Sulawesi. GPS activities in Indonesia were supported by the Dutch Integrated Solid Earth Science (ISES) research program, the French Embassy in Indonesia (Service de Coopération et d'Action Culturelles), and the French Ministry of Research (through the ACI ''Observation de la Terre'' research program). McCaffrey's participation was supported by ENS and Rensselaer Polytechnic Institute. Finally, the authors wish to thank the Jet Propulsion Laboratory for their support and advice on using the GIPSY-OASIS GPS software. This paper benefited from very constructive reviews (M. Keep, L. M. Wallace, and an anonymous Associate Editor). We want to express special thanks to L. M. Wallace for her extremely long, detailed, and thorough analysis of our work. The maps in this paper were produced using the public domain Generic Mapping Tools (GMT) software [*Wessel and Smith*, 1995].

References

Altamimi, Z., P. Sillard, and C. Boucher (2002), ITRF2000: A new release of the International Terrestrial Reference Frame for earth science applications, *J. Geophys. Res.*, *107*(B10), 2214, doi:10.1029/2001JB000561.

Aurelio, M. A. (2000), Shear partitioning in the Philippines: Constraints from Philippine Fault and global positioning system data, *Island Arc*, *9*, 584–597.

Barrier, E., P. Huchon, and M. Aurelio (1991), Philippine Fault—A key for Philippine kinematics, *Geology*, *19*, 32–35.

Beaudouin, T., O. Bellier, and M. Sebrier (2003), Present-day stress and deformation fields within the Sulawesi Island area (Indonesia): Geodynamic implications, *Bull. Soc. Geol. Fr.*, *174*, 305–317.

Bellier, O., M. Sébrier, T. Beaudouin, M. Villeneuve, R. Braucher, D. Bourlès, L. Siame, E. Putranto, and I. Pratomo (2001), High slip rate for a low seismicity along the Palu-Koro active fault in central Sulawesi (Indonesia), *Terra Nova*, *13*, 463–470.

Bellier, O., M. Sébrier, D. Seward, T. Beaudouin, M. Villeneuve, and E. Putranto (2006), Fission track and fault kinematics analyses for new insight into the Late Cenozoic tectonic regime changes in west-central Sulawesi (Indonesia), *Tectonophysics*, *413*, 201–220.

Blewitt, G., et al. (1988), GPS geodesy with centimeter accuracy, in *Lecture Notes in Earth Sciences*, vol. 19, edited by E. Groten and R. Strauss, pp. 30–40, Springer, New York.

Bock, Y., L. Prawirodirdjo, J. F. Genrich, C. W. Stevens, R. McCaffrey, C. Subarya, S. S. O. Puntodewo, and E. Calais (2003), Crustal motion in Indonesia from Global Positioning System measurements, *J. Geophys. Res.*, *108*(B8), 2367, doi:10.1029/2001JB000324.

Calmant, S., B. Pelletier, P. Lebellegard, M. Bevis, F. W. Taylor, and D. Phillips (2003), New insights on the tectonics along the New Hebrides subduction zone based on GPS results, *J. Geophys. Res.*, *108*(B6), 2319, doi:10.1029/2001JB000644.

Chamot-Rooke, N., and X. Le Pichon (1999), GPS determined eastward Sundaland motion with respect to Eurasia confirmed by earthquakes slip vectors at Sunda and Philippine trenches, *Earth Planet. Sci. Lett.*, *173*, 439–455.

Chapple, W. M., and T. E. Tullis (1977), Evaluation of the forces that drive the plates, *J. Geophys. Res.*, *82*, 1967–1984.

Chase, C. G. (1978), Extension behind island arcs and motions relative to hot spots, *J. Geophys. Res.*, *83*, 5385–5387.

DeMets, C., R. Gordon, D. Argus, and S. Stein (1990), Current plate motions, *Geophys. J. Int.*, *101*, 425–478.

DeMets, C., R. G. Gordon, D. F. Argus, and S. Stein (1994), Effect of recent revisions to the geomagnetic reversal time scale on estimates of current plate motions, *Geophys. Res. Lett.*, *21*(20), 2191–2194.

Elsasser, W. M. (1971), Sea-floor spreading as thermal convection, *J. Geophys. Res.*, *76*, 1101–1112.

Fitch, T. J. (1972), Plate convergence, transcurrent faults, and internal deformation adjacent to Southeast Asia and western Pacific, *J. Geophys. Res.*, *77*, 4432–4460.

Fitch, T. J., and W. Hamilton (1974), Reply to comment by M. G. Audley-Charles and J. Milsomon on "Plate convergence, transcurrent faults, and internal deformation adjacent to Southeast-Asia and western Pacific," *J. Geophys. Res.*, *79*, 4982–4985.

Forsyth, D., and S. Uyeda (1975), On the relative importance of the driving forces of plate motion, *Geophys. J. R. Astron. Soc.*, *43*, 163–200.

Genrich, J. F., Y. Bock, R. McCaffrey, E. Calais, C. W. Stevens, and C. Subarya (1996), Accretion of the southern Banda arc to the Australian plate margin determined by Global Positioning System measurements, *Tectonics*, *15*, 288–295.

Genrich, J. F., Y. Bock, R. McCaffrey, L. Prawirodirdjo, C. W. Stevens, S. S. O. Puntodewo, C. Subarya, and S. Wdowinski (2000), Distribution of slip at the northern Sumatran fault system, *J. Geophys. Res.*, *105*, 28,327–28,342.

Gómez, J. M., R. Madariaga, A. Walpersdorf, and E. Chalard (2000), The 1996 earthquakes in Sulawesi, Indonesia, *Bull. Seismol. Soc. Am.*, *90*, 739–751.

Hall, R. (2002), Cenozoic geological and plate tectonic evolution of SE Asia and the SW Pacific: Computer-based reconstructions, model and animations, *J. Asian Earth Sci.*, *20*, 353–431.

Hall, R., and M. E. J. Wilson (2000), Neogene sutures in eastern Indonesia, *J. Asian Earth Sci.*, *18*, 781–808.

Hamilton, W. B. (1972), Plate tectonics of Southeast Asia and Indonesia, *Am. Assoc. Pet. Geol. Bull.*, *56*, 621.

Hamilton, W. (1979), Tectonics of the Indonesian region, *U.S. Geol. Surv. Prof. Pap.*, *1078*, 345 pp. + map.

Hinschberger, F., J.-A. Malod, J.-P. Rehault, J. Dyment, C. Honthaas, M. Villeneuve, and S. Burhanuddin (2000), Origin and evolution of the North Banda Basin (Indonesia): Constraints from magnetic data, *C. R. Acad. Sci., Ser. Fasc. Sci. Terre Planètes*, *331*, 507–514.

Kato, T., J. Beavan, T. Matsushima, Y. Kotake, J. T. Camacho, and S. Nakao (2003), Geodetic evidence of back-arc spreading in the Mariana Trough, *Geophys. Res. Lett.*, *30*(12), 1625, doi:10.1029/2002GL016757.

Kreemer, C., W. E. Holt, S. Goes, and R. Govers (2000), Active deformation in eastern Indonesia and the Philippines from GPS and seismicity data, *J. Geophys. Res.*, *105*, 663–680.

Mader, G. L. (1998), GPS Antenna calibration at the National Geodetic Survey, technical report, Natl. Geod. Surv., Silver Spring, Md.

Mazzotti, S., X. Le Pichon, P. Henry, and S. Miyazaki (2000), Full interseismic locking of the Nankai and Japan-west Kurile subduction zones: An analysis of uniform elastic strain accumulation in Japan constrained by permanent GPS, *J. Geophys. Res.*, *105*, 13,159–13,177.

McCaffrey, R. (1995), DEFNODE users' guide, Rensselaer Polytech. Inst., Troy, N. Y. (Available at http://www.rpi.edu/~mccafr/defnode)

McCaffrey, R. (2002), Crustal block rotations and plate coupling, in *Plate Boundary Zones*, *Geodyn. Ser.*, vol. 30, edited by S. Stein and J. Freymueller, pp. 101–122, AGU, Washington, D. C.

McCaffrey, R. (2005), Block kinematics of the Pacific–North America plate boundary in the southwestern United States from inversion of GPS, seismological, and geologic data, *J. Geophys. Res.*, *110*, B07401, doi:10.1029/2004JB003307.

McCaffrey, R., and G. A. Abers (1991), Orogeny in arc-continent collision: the Banda Arc and western New-Guinea, *Geology*, *19*, 563–566.

McCaffrey, R., M. D. Long, C. Goldfinger, P. C. Zwick, J. L. Nabelek, C. K. Johnson, and C. Smith (2000), Rotation and plate locking at the southern Cascadia subduction zone, *Geophys. Res. Lett.*, *27*, 3117–3120.

Michel, G. W., et al. (2001), Crustal motion and block behaviour in SE-Asia from GPS measurements, *Earth Planet. Sci. Lett.*, *187*, 239–244.

Morgan, W. J. (1968), Rises, trenches, great faults, and crustal blocks, *J. Geophys. Res.*, *73*, 1959–1982.

Okada, Y. (1985), Surface deformation due to shear and tensile faults in a half-space, *Bull. Seism. Soc. Am.*, *75*, 1135–1154.

Okada, Y. (1992), Internal deformation due to shear and tensile faults in a half-space, *Bull. Seismol. Soc. Am.*, *82*, 1018–1040.

Peltzer, G., and F. Saucier (1996), Present-day kinematics of Asia derived from geologic fault rates, *J. Geophys. Res.*, *101*, 27,943–27,956.

Prawirodirdjo, L., et al. (1997), Geodetic observations of interseismic strain segmentation at the Sumatra subduction zone, *Geophys. Res. Lett.*, *24*, 2601–2604.

Prawirodirdjo, L., Y. Bock, J. F. Genrich, S. S. O. Puntodewo, J. Rais, C. Subarya, and S. Sutisna (2000), One century of tectonic deformation along the Sumatran Fault from triangulation and GPS surveys, *J. Geophys. Res.*, *105*, 28,343–28,361.

Press, W. H., B. P. Flannery, S. A. Teukolsky, and W. T. Vetterling (1989), *Numerical Recipes*, Cambridge Univ. Press, New York.

Pubellier, M., and F. Ego (2002), Anatomy of an escape tectonic zone: Western Irian Jaya (Indonesia), *Tectonics*, *21*(4), 1019, doi:10.1029/2001TC901038.

Pubellier, M., G. Girardeau, H. Permana, B. Deffontaines, M. Pubellier, and C. Rangin (1996), Escape tectonics during and after collision in western Irian Jaya, Indonesia, *Eos Trans. AGU*, *77*(46), Fall Meet. Suppl., F654.

Puntodewo, S. S. O., R. McCaffrey, E. Calais, Y. Bock, J. Rais, C. Subarya, R. Poewariardi, C. Stevens, Fauzi, J. Genrich, and P. Zwick (1994), GPS measurements of crustal deformation within the Pacific-Australia Plate boundary zone in Irian Jaya, Indonesia, *Tectonophysics*, *237*, 141–153.

Rangin, C. (1989), The Sulu Sea, a back-arc basin setting within a Neogene collision zone, *Tectonophysics*, *161*, 119–141.

Rangin, C., X. Le Pichon, S. Mazzotti, M. Pubellier, N. Chamot-Rooke, M. Aurelio, A. Walpersdorf, and R. Quebral (1999), Plate convergence measured by GPS across the Sundaland/Philippine Sea Plate deformed boundary; the Philippines and eastern Indonesia, *Geophys. J. Int.*, *139*, 296–316.

Savage, J. C. (1983), A dislocation model of strain accumulation and release at a subduction zone, *J. Geophys. Res.*, *88*, 4984–4996.

Savage, J. C., and R. O. Burford (1973), Geodetic determination of relative plate motion in central California, *J. Geophys. Res.*, *78*, 832–845.

Scherneck, H.-G. (1991), A parametrized solid Earth tide mode and ocean loading effects for global geodetic base-line measurements, *Geophys. J. Int.*, *106*, 677–694.

Silver, E. A., and J. C. Moore (1978), Molucca Sea Collision Zone, Indonesia, *J. Geophys. Res.*, *83*, 1681–1691.

Silver, E. A., R. McCaffrey, and R. B. Smith (1983a), Collision, rotation, and the initiation of subduction in the evolution of Sulawesi, Indonesia, *J. Geophys. Res.*, *88*, 9407–9418.

Silver, E. A., R. McCaffrey, Y. Joyodiwiryo, and S. Stevens (1983b), Ophiolite emplacement by collision between the Sula Platform and the Sulawesi Island-Arc, Indonesia, *J. Geophys. Res.*, *88*, 9419–9435.

Simons, W. J. F., B. A. C. Ambrosius, R. Noomen, D. Angermann, P. Wilson, M. Becker, E. Reinhart, A. Walpersdorf, and C. Vigny (1999), Observing plate motions in S.E. Asia: Geodetic results of the GEODYSSEA project, *Geophys. Res. Lett.*, *26*, 2081–2084.

Simons, W. J. F., D. L. F. van Loon, A. Walpersdorf, B. A. C. Ambrosius, J. Kahar, Z. H. Abidin, D. A. Sarsito, C. Vigny, S. Haji Abu, and P. Morgan (2000), Geodynamics of the S.E. Asia: First results of the Sulawesi 1998 GPS campaign, in *Geodesy Beyond 2000: The Challenges of the First Decade: IAG General Assembly, Birmingham, July 19–30, 1999*, *Int. Assoc. Geod. Symp.*, vol. 121, edited by K.-P. Schwarz, pp. 271–277, Springer, New York.

Socquet, A., C. Vigny, N. Chamot-Rooke, W. Simons, C. Rangin, and B. Ambrosius (2006), India and Sunda plates motion and deformation along their boundary in Myanmar determined by GPS, *J. Geophys. Res.*, *111*, B05406, doi:10.1029/2005JB003877.

Stevens, C., R. McCaffrey, Y. Bock, J. Genrich, Endang, C. Subarya, S. S. O. Puntodewo, Fauzi, and C. Vigny (1999), Rapid rotations about a vertical axis in a collisional setting revealed by the Palu Fault, Sulawesi, Indonesia, *Geophys. Res. Lett.*, *26*, 2677–2680.

Stevens, C. W., R. McCaffrey, Y. Bock, J. F. Genrich, M. Pubellier, and C. Subarya (2002), Evidence for block rotations and basal shear in the world's fastest slipping continental shear zone in NW New Guinea, in *Plate Boundary Zones*, *Geodyn. Ser.*, vol. 30, edited by S. Stein and J. Freymueller, pp. 87–99, AGU, Washington, D. C.

Tapponnier, P., G. Peltzer, A. Y. Le Dain, R. Armijo, and P. Cobbold (1982), Propagating extrusion tectonics in Asia: New insights from simple experiments with plasticene, *Geology*, *10*, 611–616.

Tregoning, P., F. K. Brunner, Y. Bock, S. S. O. Puntodewo, R. McCaffrey, J. F. Genrich, E. Calais, J. Rais, and C. Subarya (1994), First geodetic measurement of convergence across the Java Trench, *Geophys. Res. Lett.*, *21*, 2135–2138.

Tregoning, P., et al. (1998), Estimation of current plate motions in Papua New Guinea from Global Positioning System observations, *J. Geophys. Res.*, *103*, 12,181–12,204.

Tregoning, P., R. J. Jackson, H. McQueen, K. Lambeck, C. Stevens, R. P. Little, R. Curley, and R. Rosa (1999), Motion of the South Bismarck Plate, Papua New Guinea, *Geophys. Res. Lett.*, *26*, 3517–3520.

Tregoning, P., H. McQueen, K. Lambeck, R. Jackson, R. Little, S. Saunders, and R. Rosa (2000), Present-day crustal motion in Papua New Guinea, *Earth Planets Space*, *52*, 727–730.

Vigny, C., et al. (2002), Migration of seismicity and earthquake interactions monitored by GPS in SE Asia triple junction: Sulawesi, Indonesia, *J. Geophys. Res.*, *107*(B10), 2231, doi:10.1029/2001JB000377.

Wallace, L. M., C. Stevens, E. Silver, R. McCaffrey, W. Loratung, S. Hasiata, R. Stanaway, R. Curley, R. Rosa, and J. Taugaloidi (2004), GPS and seismological constraints on active tectonics and arc-continent collision in Papua New Guinea: Implications for mechanics of microplate rotations in a plate boundary zone, *J. Geophys. Res.*, *109*, B05404, doi:10.1029/2003JB002481.

Wallace, L. M., R. McCaffrey, J. Beavan, and S. Ellis (2005), Rapid microplate rotations and backarc rifting at the transition between collision and subduction, *Geology*, *33*(11), 857–860, doi:10.1130/G21834.1.

Walpersdorf, A., C. Rangin, and C. Vigny (1998a), GPS compared to long-term geologic motion of the north arm of Sulawesi, *Earth Planet. Sci. Lett.*, *159*, 47–55.

Walpersdorf, A., C. Vigny, P. Manurung, C. Subarya, and S. Sutisna (1998b), Determining the Sula Block kinematics in the triple junction area in Indonesia by GPS, *Geophys. J. Int.*, *135*, 351–361.

Walpersdorf, A., C. Vigny, C. Subarya, and P. Manurung (1998c), Monitoring of the Palu-Koro Fault (Sulawesi) by GPS, *Geophys. Res. Lett.*, *25*, 2313–2316.

Weissel, J. K., and R. N. Anderson (1978), Is there a Caroline Plate, *Earth Planet. Sci. Lett.*, *41*, 143–158.

Wells, D. L., and K. J. Coppersmith (1994), New empirical relationships among magnitude, rupture length, rupture width, rupture area, and surface displacement, *Bull. Seismol. Soc. Am.*, *84*, 974–1002.

Wessel, P., and W. H. F. Smith (1995), New version of the generic mapping tools released, *Eos Trans. AGU*, *76*(33), 329.

B. Ambrosius and W. Simons, DEOS, Delft University of Technology, Kluyverweg 1, Delft, ZH NL-2629 HS, Netherlands.

R. McCaffrey, Department of Earth and Environmental Sciences, RPI, 110 8th St., Troy, NY 12180-3590, USA.

D. Sarsito, Geodesy Research Group, Faculty of Civil and Environmental Engineering, Institute of Technology Bandung, Jl. Ganesha 10, Bandung 40132, Indonesia.

A. Socquet, Department of Earth and Space Sciences, University of California, 595 Charles E. Young Drive East, Los Angeles, CA 90095-0000, USA. (socquet@ucla.edu)

W. Spakman, Faculty of Earth Sciences, Utrecht University, Budapestlaan 4, NL-3584 CD, Utrecht, Netherlands.

C. Subarya, BAKOSURTANAL, Jl. Raya Jakarta-Bogor KM46, Cibinong, 16911, Indonesia.

C. Vigny, Laboratoire de Géologie, Ecole Normale Supérieure, UMR CNRS 8538, 24 rue Lhomond, F-75231 Paris cedex 05, France.